Ternary Complex Formation and Induced Asymmetry in Orotate Phosphoribosyltransferase[†,‡]

Lilian González-Segura,[§,||] John F. Witte,[⊥] Ronald W. McClard,[⊥] and Thomas D. Hurley*[,§]

Department of Biochemistry and Molecular Biology, Indiana University School of Medicine, Indianapolis, Indiana 46202, and Arthur F. Scott Laboratory of Chemistry, Reed College, Portland, Oregon 97202

Received May 25, 2007; Revised Manuscript Received October 12, 2007

ABSTRACT: Orotate phosphoribosyltransferase (OPRTase, EC 2.4.2.10) catalyzes the Mg^{2+}-dependent condensation of orotic acid (OA) with PRPP (5-α-D-phosphorylribose 1-diphosphate) to yield diphosphate (PP_i) and the nucleotide OMP (orotidine 5′-monophosphate). We have determined the structures of three forms of *Saccharomyces cerevisiae* OPRTase representing different structural and enzymatic intermediates. The structures include the apoenzyme (2.35 Å resolution); a ternary complex of enzyme, Mg^{2+}-PRPP, and OA (1.74 Å resolution); and the binary product complex of enzyme with OMP (1.89 Å resolution). While the overall structure of the *S. cerevisiae* OPRTase is similar to that of the *Salmonella typhimurium* enzyme, as judged by comparison of the two apoenzymes, large conformational transitions occur proceeding from the apoenzyme structure to those of the substrate and product complexes. Comparison of these structures reveals a rotation of the upper hood domain onto the bound ligands by an average of 19.5° in the OMP structure and an average of 24.6° in the OA/Mg^{2+}-PRPP ternary complex. As expected, the conserved loop, composed of residues 104−116, moves extensively and adopts a single stable conformation during the catalytic cycle in order to sequester the substrates from bulk solvent in the ternary complex. The OA and Mg^{2+}-PRPP molecules bound in the ternary complex are oriented for proper attack of the N1 atom of OA onto the C1 atom of the ribose ring. This orientation of substrates, combined with the positioning of the flexible loop, provides a clear picture of a catalytically poised reaction complex for type I phosphoribosyltransferases. The structural asymmetry present in these structures, as well as that found in a recent structure of the *S. typhimurium* enzyme, combined with the closure of the flexible loop from one subunit into the active site of the opposing subunit in the ternary complex is consistent with the kinetic data [McClard, R. W., et al. (2006) *Biochemistry 45*, 5330−5342] that demonstrate induced nonequivalence and cooperativity of OPRTase.

Phosphoribosyltransferases (PRTases)[1] play an essential role in both de novo and recycling pathways of purine, pyrimidine, and pyridine metabolism as well as in the biosynthesis of histidine and tryptophan. PRTases constitute two evolutionary families, designated types I and II, characterized by distinct folding architectures. In particular, orotate phosphoribosyltransferase (OPRTase) from the type I family catalyzes the Mg^{2+}-dependent condensation of orotic acid (OA) with PRPP (5-α-D-phosphorylribose 1-diphosphate) to yield PP_i and the nucleotide orotidine 5′-monophosphate (OMP), which is converted by OMP decarboxylase to uridine 5′-monophosphate (UMP), the entry nucleotide to *de novo* biosynthesis of all the pyrimidine nucleotides. In humans, the OPRTase reaction serves to activate the prodrug 5-fluorouracil (*1*), while inherited defects in the nucleotide synthases lead to severe inborn disorders of metabolism, including orotic aciduria (*2*), 2,8-dihydroxyadenine lithiasis (*3*), and Lesch−Nyhan syndrome (*4*). The enzymes are also direct targets for inhibiton of cell growth, which has found use in antiparasitic therapies (*5*, *6*).

Saccharomyces cerevisiae OPRTase, a homodimer, is a typical example of the type I PRTase family, and its kinetic mechanism has been the subject of several studies. The initial investigation led to the conclusion that the enzyme proceeds through an oxocarbenium transition-state/high-energy intermediate as evidenced by observed isotope effects (*7*). That concept was built upon when it was concluded from both a kinetic evaluation and equilibrium isotope exchange studies that the enzyme followed a Ping-Pong Bi-Bi mechanism, with PRPP binding first to the enzyme followed by the release of PP_i to yield an enzyme-bound phosphoribosyl oxocarbenium intermediate (*8*). The Ping-Pong mechanism was later ruled out when the equilibrium exchange studies were revisited by magnetization transfer with enzyme that had been completely freed of "tightly bound" OMP (*9*). A

[†] This work was supported by a grant from the National Institutes of Health (R15GM61317, to R.W.M.).

[‡] Coordinates and structure factors have been deposited in the RCSB Protein Data Bank under codes 2PRY, 2PRZ, and 2PS1.

* To whom correspondence should be addressed: tel 317-278-2008; fax 317-274-4686; e-mail thurley@iupui.edu.

[§] Indiana University School of Medicine.

[||] Present address: Departamento de Bioquimica, Facultad de Quimica, Universidad Nacional Autonoma de Mexico, Mexico D.F. 04510, Mexico.

[⊥] Reed College.

[1] Abbreviations: PRTases, phosphoribosyltransferases; OPRTase, orotate phosphoribosyltransferase (EC 2.4.2.10); OA, orotic acid; PRPP, 5-α-D-phosphorylribose 1-diphosphate; OMP, orotidine 5′-monophosphate; PPi, diphosphate; UMP, uridine 5′-monophosphate; GPATase, glutamine phosphoribosylpyrophosphate amidotransferase (EC 2.4.2.14); HGPRTase, hypoxanthine phosphoribosyltransferase (EC 2.4.2.8).

10.1021/bi701023z CCC: $37.00
Published on Web 11/20/2007

more recent study proposed an enzymatic mechanism that is consistent with an alternating sites model of catalysis in which there is essentially cotemporal binding of OA and dissociation of PP_i, by adapting a Theorell−Chance mechanism in which 1 equiv of OMP or PRPP binds at any given time across the two identical subunits in a highly cooperative fashion in which free enzyme does not participate within the catalytic cycle (*10*). In contrast, the *Salmonella* enzyme was shown to operate by a random ordered mechanism (*11*).

Prior crystallographic structures of bacterial OPRTases have revealed a conserved Rossmann nucleotide binding fold with a variant "hood" structure that provides for binding of OA along with partial solvent occlusion (*12*, *13*). The most obvious feature of these structures is that the remainder of the active site is relatively solvent-exposed. Thus the reactive center, C1 of bound PRPP or C1′ of OMP, is directly accessible to solvent (*12*, *13*), implying that some conformational event must occur to generate a solvent-occluded active site. The observation of such an event in OPRTase from *Salmonella* is available from one structure deposited in the Protein Data Bank but, as of yet, not described in a paper.[2] Adjacent to the active site in all type I PRTases is a solvent-exposed loop whose high temperature factors in crystallographic studies indicate conformational flexibility. The motional dynamics of this loop segment from NMR and proteolysis are in accord with the loop being highly flexible in the unliganded enzyme from *Salmonella* (*14*). In other cases the loop has been visualized in conformations that overlie the active site (*15*), particularly with glutamine phosphoribosylpyrophosphate amidotransferase (GPATase), where the loop has been captured in a down position atop an active site occupied by a carbocyclic PRPP analogue (*16*).

Here we report the three-dimensional structures of OPRTase from *S. cerevisiae* in three distinct enzymatic species; the apo form, a ternary complex with substrates Mg^{2+}-PRPP and OA, and in a binary OMP product complex. The structures provide clear evidence for a large conformational change associated with ligand binding as well as a ternary complex-dependent recruitment of the flexible loop into the active-site environment to both engender solvent exclusion and contribute conserved residues that serve to stabilize the transition state of the enzymatic reaction.

EXPERIMENTAL PROCEDURES

Materials. OMP was synthesized by published methods (*10*). Buffers, PRPP, $MgCl_2$, and other reagent-grade biochemicals were obtained from Sigma Chemical Co. OA was purchased from Acros Organics. Poly(ethylene glycol) 6000 and 4000 were from Fluka, and the 24-well sitting drop trays were from Charles Supper Co., Inc. (Natick, MA).

OPRTase Purification. OPRTase was overexpressed, purified, and assayed by published procedures (*9*). Protein concentrations for kinetic studies were determined by dry-weight analysis (*10*) or the bicinchoninic acid (BCA) assay (Pierce Chemical Co.). For the purposes of crystallization experiments, protein concentration was estimated by the method of Bradford (*17*) by use of a Bio-Rad protein assay reagent kit and bovine serum albumin as a standard.

Crystallization. Crystals of OPRTase were grown by vapor diffusion with the sitting drop configuration. The drops were set up with 2 μL of protein plus 2 μL of the precipitant solution. The protein concentrations were 15 mg/mL, and crystals were harvested within 2−3 weeks. The apoenzyme crystallized from solutions containing 100 mM Tris-HCl, pH 7.4, 0.2 M magnesium acetate, and 26% (w/v) PEG 6000. Crystals of OPRTase in complex with substrates (5.0 mM PRPP and 5.0 mM OA) or product (5.0 mM OMP) were obtained by adding these compounds, as well as 2.0 and 2.5 mM $MgCl_2$, respectively, directly to the protein solution prior to crystallization. The crystals of the ternary complex were grown from solutions containing 100 mM sodium acetate, pH 4.6, 0.14 M ammonium acetate, and 38% (w/v) PEG 4000. The crystals of the OMP complex were grown from solutions containing 100 mM Tris HCl, pH 7.4, 0.08 M magnesium acetate, and 28% (w/v) PEG 6000. Trays yielding the product and apoenzyme crystals were incubated at 20 °C, while the ternary complex crystals were obtained at 15 °C.

Data Collection, Processing, and Model Refinement. Diffraction data were collected on a Rigaku H2R rotating-anode generator, equipped with a Raxis IV^{++} and Osmic Confocal optics (apoenzyme), and at the Advanced Photon Source (APS) at Argonne National Laboratory (Argonne, IL) on beamline SBC-CAT 19-ID (binary and ternary complexes). The Raxis IV^{++} home data were processed and scaled by use of the d*TREK program (*18*), and the data collected at beamline 19-ID were processed and scaled by use of the HKL2000 program suite (*19*). All the structures were solved by molecular replacement with the programs AMoRe (*20*) and Molrep (*21*), as implemented in the CCP4 program package (*22*). The original apoenzyme form of the *Salmonella typhimurium* OPRTase enzyme served as the search model (Protein Data Bank code 1STO) for the apoenzyme structure, while the refined *S. cerevisiae* apoenzyme structure served as the search model for the binary and ternary complexes. Alternating cycles of automatic and manual refinement were carried out via the simulated annealing, minimization, and individual temperature factor refinement protocols as implemented in the Crystallography and NMR System program suite (CNS, version 1.1) (*23*). Visual inspection and manual correction of the resulting model structures were accomplished by using the program package O (*24*) and the program Coot (*25*). All structures showed evidence of a non-proline cis-peptide bond between residues Ala74 and Tyr75. Consequently, parameters were introduced into the refinement protocols to maintain this unusual peptide bond conformation. Parameters for proper stereochemical refinement of the bound OMP and the bound OA and Mg^{2+}-PRPP were developed from the HIC-UP site (*26*) and modified for use in our refinement protocols.

Structure Analysis. The conformational differences between OPRTase with and without bound ligands were analyzed with the program DynDom (*27*) as implemented in the CCP4 package. Additional domain alignments were performed with the program LSQKAB (*28*) as implemented in the CCP4 package. Root-mean-square deviations were calculated for the Cα atoms for each alignment. Molecular figures were created with PyMOL (*29*), Swiss PDB Viewer (*30*), and POV-Ray (*31*).

[2] PDB code 1LH0 is the crystal structure of *Salmonella typhimurium* OMP synthase in a complete substrates complex; A. A. Federov, K. Panneerselvam, W. Shi, C. Grubmeyer, and S. C. Almo.

Site-Directed Mutagenesis. Mutants of "wild-type" yeast OPRTase were created with the pREJ2 plasmid (*9*) as template and the Stratagene Ex-Site kit. Appropriate synthetic DNA single-strand oligonucleotides were produced to create A661C, A664C, and A661C/A664C (double) mutations, which resulted in D131A, D132A, and D131A/D132A substitutions when translated.[3] Screening of potential clones was facilitated by the consequence that the A661C mutation resulted in the loss of one of two *Tth*111I restrictions sites, while A664C resulted in loss of a unique *Aat*II site. The sequences of mutated plasmids were verified by DNA sequencing at the Oregon Health and Sciences University. During the course of sequence verification it was learned that pREJ2 ("wild-type") plasmid, and all derived plasmids, bear a G715A mutation which results in a benign S149N mutation, relative to the parent DNA construct in a nonconserved region of the enzyme (*32*). The mutated plasmids were transformed into $CaCl_2$-competent cells of the *pyrE- E. coli* strain CS101-4UI, and OPRTase was expressed and purified as previously described (*9*).

RESULTS

Structure Determination and Quality. The three-dimensional structures of OPRTase from *S. cerevisiae*, the free enzyme, ternary complex (OPRTase and the substrates PRPP and OA), and binary complex (OPRTase and OMP) have been solved. The crystals of the apoenzyme belong to the tetragonal ($P4_32_12$) space group and contain one monomer in the asymmetric unit. The ternary complex formed in the triclinic ($P1$) space group, diffracted anisotropically to 1.74 Å resolution, and contains a dimer in the asymmetric unit. The binary complex with OMP formed in the orthorhombic ($P2_12_12_1$) space group with two dimers in the asymmetric unit and diffracted anisotropically to 1.89 Å resolution. Data collection and refinement statistics are summarized in Table 1. The structures have a minimum of 93% of their residues in the most favored region of their respective Ramachandran plots; only Glu203 of monomer B in the binary complex was in a disallowed region.

Overall Description of the Structures. The monomer of *S. cerevisiae* OPRTase contains 225 residues and is composed of 10 β-strands (B1−B10), seven regular α-helices (A1−A7), and a single turn of a 3_{10}-helix between A2 and B4 for the free enzyme (Figure 1A). In the ternary complex, the B7 β-strand is better defined as a loop structure; a similar shift in secondary structure assignment also occurs in the OMP complex (Figure 1B). Apart from the nine β-strands, the seven regular α-helices, and a single turn of a 3_{10}-helix, one new single-turn 3_{10}-helix is found in the binary complex between A3 and B6 (Figure 1C). These elements of secondary structure are similar, as are the overall structures, to that of *S. typhimurium* OPRTase (*12, 13*).

The protein can be divided into the same three structural regions defined in the *S. typhimurium* enzyme: N-terminal, core, and C-terminal regions. In the structure of the ternary complex, the N-terminal region (residues 2−42) contains the same regular α-helix, a single turn of a 3_{10}-helix, and four short antiparallel β-strands that were shown in *S. typhimurium*. Two of these β-strands in the N-terminal region are known as the "hood" (*12, 13*) and partially envelop the OA ring in the ternary complex. The core region (residues 43−192) shows a topology similar to the dinucleotide binding fold found in many dehydrogenases (*33*) and contains a five-stranded twisted β-sheet, instead of the four found in *S. typhimurium* enzyme, surrounded by four α-helices. The C-terminal region (residues 193−225) is composed of two antiparallel α-helices connected by a loop structure that is longer in the *S. cerevisiae* enzyme. The core region can be divided into two similar halves; the first half contains two parallel β-strands and one α-helix and is connected to the second half by a long flexible loop composed of residues 104−116 (Ala102−Arg119 in *S. typhimurium*). Residues 109−114 (103−107 in *S. typhimurium*) of this loop are surface-exposed and of variable position in different substrate/product complexes.

Table 1: Data Collection and Refinement Statistics

	apo-OPRTase	OPRTase−OA-PRPP	OPRTase−OMP
space group	$P4_32_12$	$P1$	$P2_12_12_1$
cell dimensions			
a, *b*, *c* (Å)	60, 60, 135	42, 50, 50	86, 99, 112
α, β, γ (deg)	90, 90, 90	90, 106, 93	90, 90, 90
asymmetric unit	monomer	dimer	two dimers
resolution (Å)	24.92−2.35	49.96−1.74	74.37−1.89
total observations	66 930	132 897	378 313
unique reflections	10 718	36 660	74 091
completeness (%)	98.5 (84.5)	92.9 (63.7)	95.2 (66.4)
$I/\sigma(I)$	24.4 (3.7)	17.8 (3.2)	11.7 (2.4)
R_{merge}	0.053 (0.25)	0.049 (0.25)	0.053 (0.42)
R_{work} (%)	23.8	19.4	22.9
R_{free} (%)	26.0	21.7	26.2
total atoms	1764	3836	7315
solvent atoms	100	322	447
avg *B* value (Å^2)			
protein	49.49	22.98	29.71
solvent	51.27	31.90	35.14
magnesium	61.81	19.78	
PRPP		16.38	
OA		15.79	
OMP			25.18
PDB ID code	2PRY	2PS1	2PRZ

Residues 109−114 exhibit weak or nonexistent ($F_o - F_c)\alpha_{calc}$ electron density in the apoenzyme structure and are not present in the final refined model. Similarly, the electron density is weak for residues 109−114 in the A and C subunits and for residues 109−115 in the B and D subunits of the OMP complex. In contrast, this loop is well-ordered and in position to interact with the bound PRPP molecule present in the ternary complex (Figure 2). This interaction occurs across the subunit interface such that residues within this loop contact the PRPP molecule bound in the opposing subunit. These results suggest that this loop is critical for formation of a productive catalytic complex but has little role in binding OMP.

Binding of OA and PRPP. One molecule of OA and one molecule of PRPP were bound per monomer in the ternary complex (Figure 3A). The OA ring lies parallel to and stacked against the phenyl ring of Phe37; its O4 atom hydrogen bonds to the main-chain nitrogen of Phe38 and to

[3] The *Saccharomyces* URA5 gene sequence (*32*; see also locus X14795 at www.ncbi.nlm.nih.gov/entrez), cloned to form plasmid pREJ2 (*9*) in our work, has the ORF for OPRTase beginning at bp 1114 which corresponds to bp 267 in plasmid pREJ2. The mature OPRTase lacks the leading Met residue, so numbering in this paper begins with Pro2 as the first amino acid residue Pro1, etc.

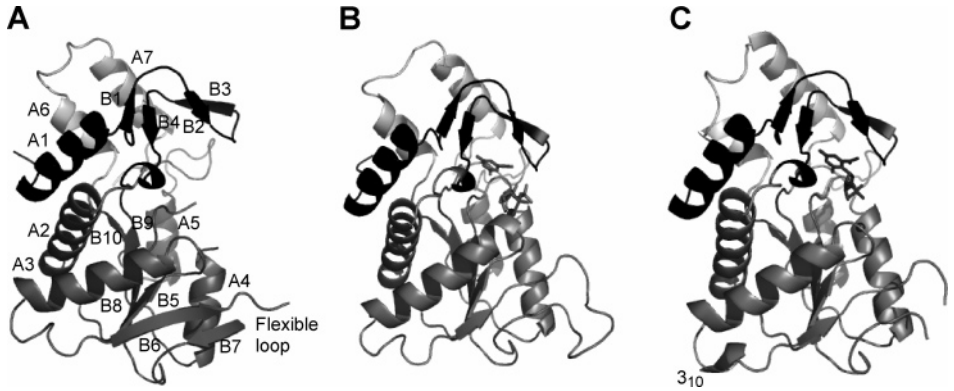

FIGURE 1: Ribbon diagram of the three-dimensional structures of *S. cerevisiae* OPRTase. The three segments of the OPRTase structure are illustrated as N-terminal region (black), core region (gray), and C-terminal region (light gray). (A) Structure of the single subunit present in the apo-OPRTase crystal. (B) Structure of one monomer from the dimeric ternary complex structure of OPRTase. (C) Structure of one monomer from the OPRTase structure with bound OMP. Bound substrates or products present in each structure are shown in ball-and-stick representation.

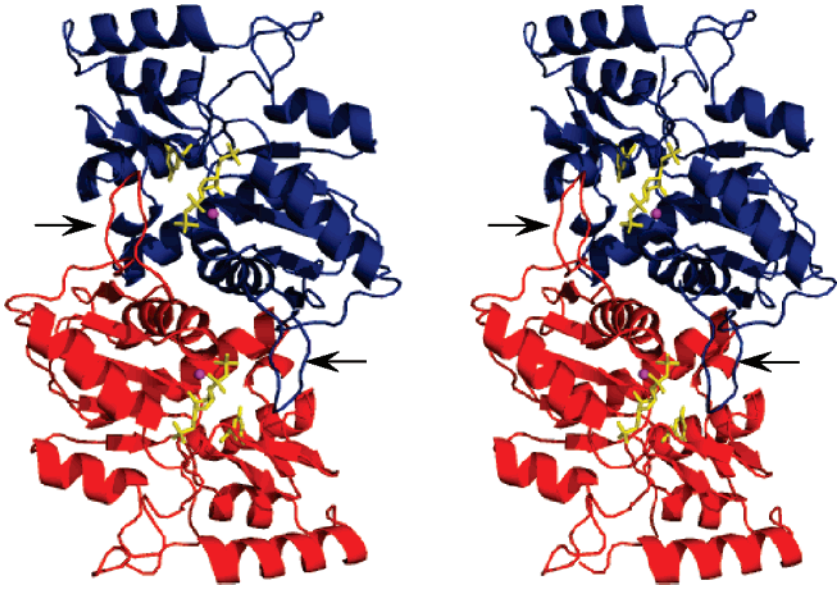

FIGURE 2: Ribbon diagram in stereo of the functional dimer of *S. cerevisiae* OPRTase in the ternary complex, with individual subunits colored blue (subunit A) and red (subunit B). Bound substrates (OA and PRPP) are shown in yellow ball-and-stick representations, and the Mg^{2+} is displayed as magenta spheres. Arrows indicate locations of the flexible loops.

a guanidinium of Arg163 (Figure 3B). The N3 atom of OA hydrogen-bonds to the main-chain oxygen of Phe38, and the carboxylate hydrogen-bonds to the OG1 of Thr135, the main-chain nitrogen of Lys29, and two ordered water molecules located in the active site. The orotate O2 atom hydrogen-bonds to two ordered water molecules located in the active site, which are in turn hydrogen-bonded to Lys76, Lys109, and Asp132 (Figure 3B).

The 5-phosphate of PRPP is located within a conserved PRPP-binding motif formed by residues 133−138 (Figure 3C), which are equivalent to residues 126−131 in the *S. typhimurium* enzyme (*13*). These residues exhibit well-defined electron density in both our binary and ternary complexes, but our apoenzyme structure shows discontinuous electron density for the main-chain atoms within this stretch of residues. The three oxygens of the 5-phosphate of PRPP form an extensive network of hydrogen bonds with main-chain nitrogens of Thr135, Ala136, Gly137, and Ala139 and to the side-chain nitrogen of Lys29 (Figure 3C).

The ribose hydroxyl groups of PRPP form hydrogen bonds with two conserved aspartate residues, Asp131 and Asp132. The O3 hydroxyl group forms a hydrogen bond with Asp131 and the O2 hydroxyl group forms two partial hydrogen bonds with Asp132. The diphosphate α-phosphate oxygen atoms interact with the side-chain nitrogen of Lys109 of the opposing subunit along with four water molecules, while the *β*-phosphate oxygen atoms interact with the guanidinium group of Arg105 and the imidazole of His111 located in the flexible loop emanating from the other subunit as well as the main-chain nitrogen atoms of Lys76 and Tyr75 (Figure 3C). An unusual non-proline cis-peptide bond occurs between Tyr75 and Lys76.

Binding of OMP. One molecule of OMP is bound per monomer in our binary complex (Figure 4A). The OA group of OMP is located in a solvent-inaccessible crevice formed by residues from the core and hood domains and is in a similar position in the *S. typhimurium* structure (*13*). As observed in the ternary complex, the OA ring is stacked under the phenyl ring of Phe37, and N3 and O4 atoms interact with Phe38 and the side-chain nitrogen of Arg163 in a similar manner. The carboxylate group of the OA moiety also forms similar interactions with the main-chain nitrogen

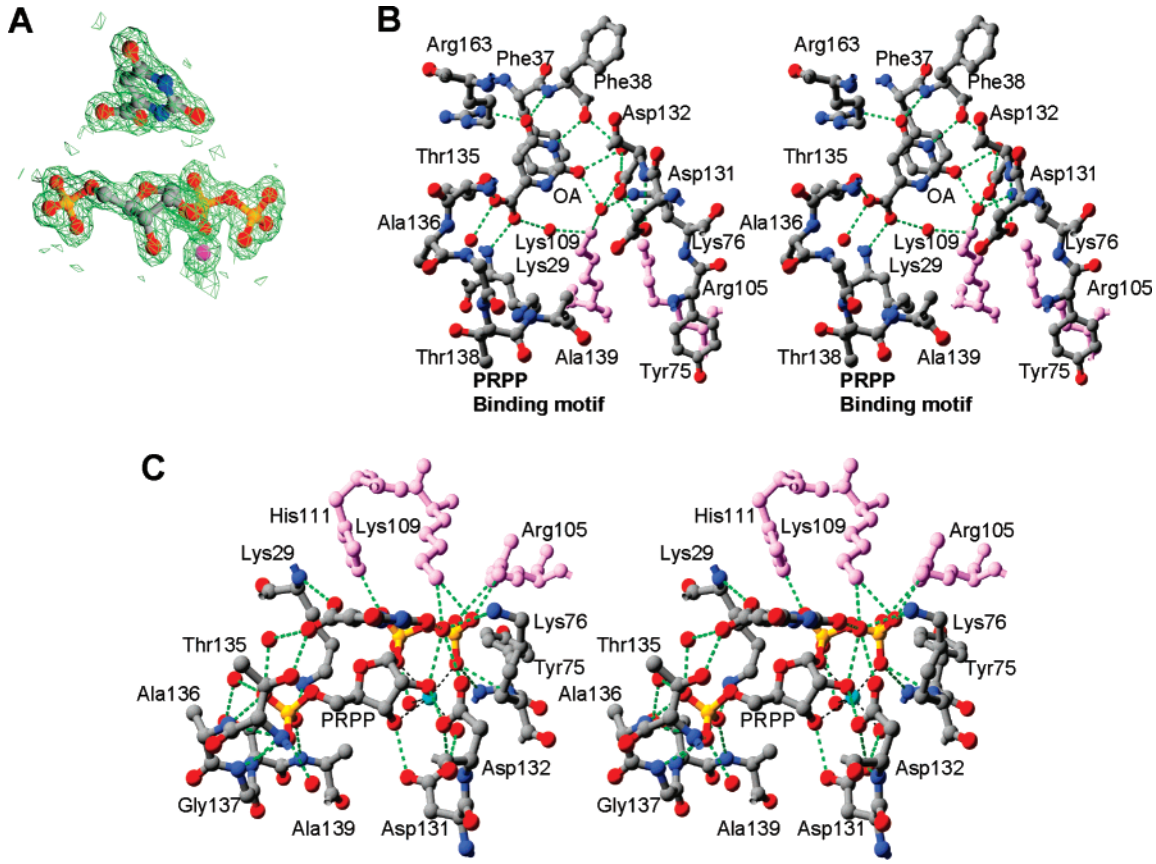

FIGURE 3: *S. cerevisiae* OPRTase active site in the ternary complex. (A) A σ_A-weighted $2F_o - F_c$ electron density map contoured at 1.5 standard deviations of the map for the bound OA, PRPP, and Mg^{2+} molecules. For all figures, the atoms from OPRTase are shown in ball-and-stick representations and atom-type coloring with carbon in gray, nitrogen in blue, oxygen in red, phosphorus in orange, and magnesium in magenta, except as otherwise noted, (B) Stereoview of the interactions between the active-site residues of OPRTase and OA (ball-and-stick representation). Residues contributed by the opposing subunit are colored pink. (C) Stereoview of the interactions between the active-site residues of OPRTase and PRPP (ball-and-stick model).

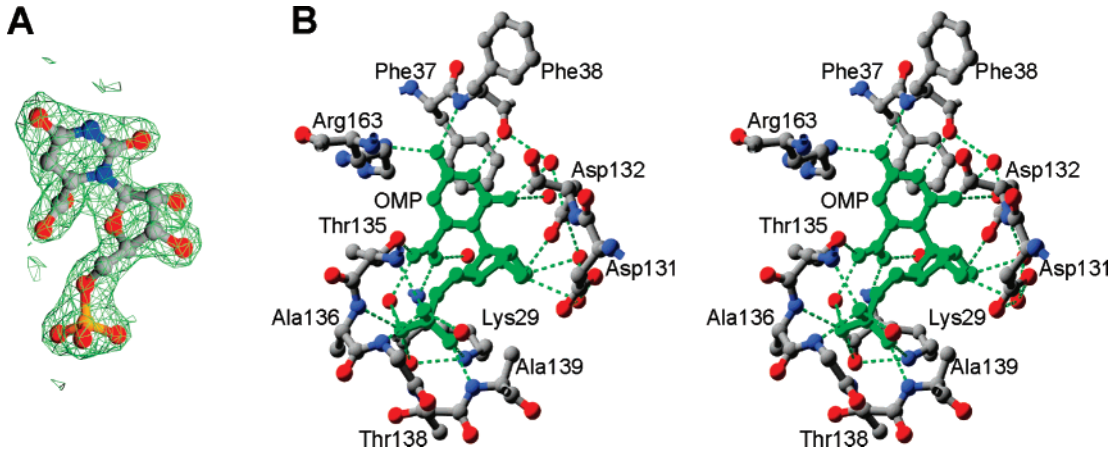

FIGURE 4: *S. cerevisiae* OPRTase active site in the binary OMP complex. (A) A σ_A-weighted $2F_o - F_c$ electron density map contoured at 1.5 standard deviations of the map for the bound OMP and Mg^{2+} molecules. (B) Stereoview of the residues involved in the OMP (ball-and-stick model) binding.

of Lys29, the side chain of Thr135, and two ordered water molecules. The OA C5 atom is located in the tightly packed crevice near Arg163 and the protein backbone. The O2′ and O3′ ribose hydroxyl groups form hydrogen bonds with the side chain of Asp132 and with one ordered water molecule. The 5′-phosphate of OMP is located in the same pocket (Val133−Thr138) that held the 5-phosphate of PRPP, with the three oxygens forming an extensive network of hydrogen bonds with main-chain nitrogens of Thr135, Ala136, Gly137, and Ala139 as well as to the side-chain nitrogen of Lys29 (Figure 4B).

Binding of Mg^{2+}. The OPRTase reaction requires Mg^{2+} ions (*34*), in which the Mg^{2+} was found to form a complex with PRPP. In the case of *S. cerevisiae* OPRTase, PRPP does not bind to the enzyme in the absence of Mg^{2+} (*10*). In the ternary complex a Mg^{2+} is found in nearly octahedral coordination: two of these interactions involve the ribose hydroxyls, two more are contributed by the oxygens of the

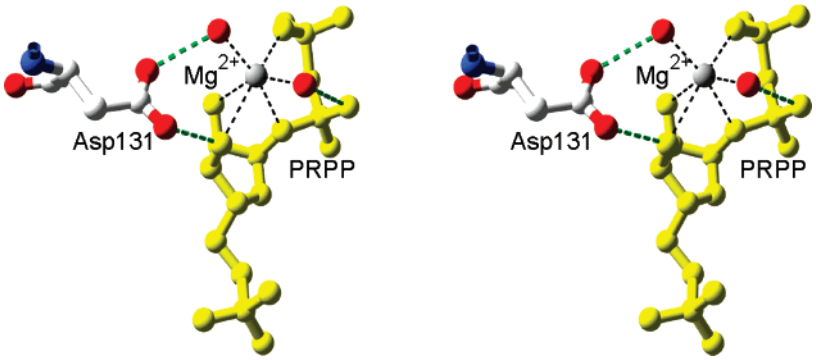

FIGURE 5: Stereo diagram of the interactions surrounding the Mg^{2+} ions in *S. cerevisiae* OPRTase. Interactions between Mg^{2+} (gray) PRPP (yellow), and Asp131 (atom-type coloring) in the ternary complex structure are shown.

Table 2: Kinetic Constants for *S. cerevisiae* OPRTase and Mutants

	K_m^{OMP} (μM)	K_m^{PRPP} (μM)	sp act. (μmol min^{-1} mg^{-1})
wild type	4.0 ± 1.0	41± 4.0	38 ± 1
D131A	7.0 ± 2.0	43 ± 5.0	0.35 ± 0.03
D132A	7.0 ± 1.0	120 ± 12	0.30 ± 0.01
D131A132A	10 ± 2.0	86 ± 20	0.040 ± 0.003

diphosphate moiety, and the remaining two are provided by two water molecules (Figure 5).

Mutagenesis Results. Mutation of the conserved aspartate residues (131 and 132) to alanine lead to relatively small changes (2−3-fold) in the Michaelis constants for PRPP and OMP yet 100−1000-fold changes in specific activity (Table 2). In the ground-state product complex and the catalytically poised but ground-state ternary complex, Asp 131 and Asp132 form hydrogen bonds with the 3′- and 2′-hydroxyl groups of the ribose moiety, respectively. These hydrogen bonds apparently contribute relatively little to the free energy of substrate/product binding, but their importance during catalysis is clearly shown by the large reductions in specific activity, suggesting a role in stabilizing an oxocarbenium transition state of the reaction.

DISCUSSION

The crystal structure of apo *S. cerevisiae* OPRTase reveals that the enzyme undergoes two distinct changes in structure accompanying the formation of a catalytically poised ternary complex and the OMP complex. The two changes encompass rigid-body rotations of domains along with a disorder-to-order transition of loop residues 104−116, a consequence of the fact that the loop becomes well-ordered only when poised to interact with the bound PRPP molecule in the opposing subunit of the ternary complex. The hydrogen bonds contributed by residues Arg105, Lys109, and His111 to PRPP serve to stabilize the loop in the closed conformation (Figure 3B), and sequester the substrates from bulk solvent. This change is reminiscent of those found in the *E. coli* GPATase in a complex with a nonreactive PRPP analogue (*16*) and in human hypoxanthine phosphoribosyltransferase (HGPRTase) complexed with a hypoxanthine analogue and PRPP (*35*), which also revealed a loop-down structure. The structural rearrangements in HGPRTase are brought about by residue Tyr104, which interacts with the 5-phosphate moiety of PRPP such that the side chain is positioned over the O4 atom of the PRPP ribose moiety (*35*).

In published structures of OPRTase from *S. typhimurium*, including those containing substrate or product, the loop exhibited considerable flexibility. However, a structure recently deposited in the Protein Data Bank (1LH0)[2] shows a closed loop conformation and domain rotation in one of the subunits that is very similar to what we observe in both subunits of our ternary complex. Like 1LH0, the structure of *Escherichia coli* OPRTase in complex with an inhibitor found one loop in a down position over the active site of the adjacent subunit, while the other loop remained extended into the solvent (*36*). A similar disparity in the loop conformation was observed in the structure of *Trypanosoma cruzi* HPRTase in complex with PRPP and an analogue of the substrate hypoxanthine (*37*). Thus, it would appear that this loop structure can adopt a variety of conformations, but the formation of complexes similar to that of our quasi-catalytic ternary complex fixes its position.

In addition to the ordering of the flexible loop structure upon ternary complex formation, the binding of both substrates or of the product OMP induced rigid-body rotations of secondary structure elements in OPRTase. When the program DynDom was used to compare the apo-OPRTase structure to the ternary and binary complex structures, two rigid-body domains were identified. The first domain, or the "fixed" domain, is composed of approximately 158 amino acid residues and the second, or "moving", domain contains approximately 51 residues composed of the four short antiparallel β-strands (residues 20−38) of the N-terminal region which includes the previously described "hood domain", one loop (residues 165−166 in the ternary complex, as well as residues 170−174 in the binary complex), and two antiparallel α-helices (residues 198−221) from the C-terminal region (Table 3). The analysis uses the "fixed domain" as a structural reference point and then calculates the extent of rotation and translation to be applied to the "moving domains" for their superposition. As a consequence of substrate and product binding, the enzyme undergoes a conformational change where the moving domain rotates down on top of the bound ligands by an average of 19.5° for the binary OMP complex and 24.6° for the ternary complex (Table 3 and Figure 6A,B).

The more extensive domain closure in the ternary complex facilitates both the capture of the substrates in a catalytically competent position and the sequestering of the reactants from bulk solvent. The intermediate domain position in the OMP complex, combined with the local disorder of the flexible

Table 3: Analysis of Domain Motion in OPRTase from *S. cerevisiae*[a]

	subunits			
	A	B	C	D
Ternary Complex vs Apoenzyme				
domain 1 (fixed)				
residue range	5−19	5−19		
residue range	39−163	39−162		
residue range	167−197	167−194		
domain 2 (moving)				
residue range	4−4	4−4		
residue range	20−38	20−38		
residue range	164−166	163−166		
residue range	198−223	195−223		
rotation angle (deg)	22.1	27.1		
translation (Å)	0.3	−0.1		
Binary Complex vs Apoenzyme				
domain 1 (fixed)				
residue range	5−19	5−19	5−19	5−19
residue range	39−164	39−164	39−164	39−164
residue range	167−169	167−169	167−169	167−169
residue range	175−196	175−197	175−196	175−197
residue range	222−222	222−222		222−222
domain 2 (moving)				
residue range	20−38	4−4	20−38	4−4
residue range	165−166	20−38	165−166	20−38
residue range	170−174	165−166	170−174	165−166
residue range	197−221	170−174	197−222	170−174
residue range		198−221		198−221
rotation angle (deg)	19.7	18.9	20.8	18.7
translation (Å)	0.4	0.4	0.4	0.4

[a] All results were produced withg the program DynDom (*27*).

loop structure, enables the products to be released from the active site following the completion of the reaction (Figure 6B). The closed domain position observed in the ternary complex and the interactions provided by the now-ordered flexible loop to the PRPP molecule create the proper orientation and proximity for the N1 atom of OA to attack the C1 atom of the PRPP molecule and to sequester the nascent oxocarbenium transition state from counterproductive interaction with bulk solvent. The extensive contacts between the flexible loop and the PRPP molecule, as well as with the "hood" domain of OPRTase, appear to stabilize this more "closed" domain position. On a related note, the addition of OMP or OA and Mg^{2+}-PRPP to the apoenzyme crystals resulted in shattering of the lattice. Thus, the free energy associated with these new contacts and resulting conformational changes appears to overwhelm the lattice forces in the apoenzyme crystals. Thus, the underlying structural changes necessitated the search for separate cocrystallization conditions compatible with each of the complexes.

A comparison of the *S. cerevisiae* OPRTase ternary and binary complex structures shows that the protein maintains a similar overall structure in the two complexes but exhibit a relatively large rms difference of 0.6 Å for their respective Cα atoms, a consequence of an approximate 5° rotational difference in their "hood domains" (Figure 6B). When aligned in this manner, the free OA and the OA moiety of OMP occupy similar positions within the protein and maintain the same points of contact with the surrounding amino acid residues. The position of the 5′-phosphate moiety is also similar in the binary and ternary complexes, where the 5′-phosphate is located in the phosphate binding loop composed of residues 133−138. The numbers of hydrogen bonds formed between the 5′-phosphate and protein atoms are the same in both complexes. The ribosyl group shows the largest difference in position between the two complexes: in the ternary complex, it is located about 2.5 Å away from its position in the OMP structure (Figure 6C).

The OA and Mg^{2+}-PRPP molecules in the ternary complex are oriented for proper attack of the N1 atom on the C1 atom of the ribose ring (Figures 3C and 6C). The reaction catalyzed by OPRTase proceeds with inversion of configuration at the anomeric carbon (*38*). An S_N1-like mechanism via an oxocarbenium intermediate has been proposed for the yeast enzyme on the basis of primary and secondary isotope effect studies (*7*), and a loosely associative oxocarbenium-like transition state for phosphoribosyl transfer has been demonstated for the *Salmonella* enzyme (*39*). The generation of the oxocarbenium transition state would come about following lengthening of the C1−O1 bond in the PRPP molecule in the forward reaction or the C1′−N1 bond in OMP in the reverse reaction. It is intriguing that the reaction has not occurred in this ternary complex, even though the distance between the N1 and the C1 atoms is, on average, only 4.1 Å. A possible reason for the lack of catalysis is that the low pH of the crystallization solution (pH 4.6) prevents formation of the nucleophilic form of the N1 atom through deprotonation of the OA ring. One likely chemical mechanism for activation of the N1 atom is the stabilization of the tautomer of OA in which the O2 atom exists in its hydroxyl form in the enzyme active site. On the basis of measured and calculated kinetic isotope effects for *Salmonella* OPRTase, Tao et al. (*39*) concluded that a well-accepted oxocarbenium intermediate must exist and that the transition state of the rate-determining step resembles product OMP. The consequence of this chemical mechanism is that a major role in catalysis is assigned for the abstraction of a proton from OA (presumably the C2-OH of the N1−C2 iminol tautomer) to activate the subsequent formation of OMP (Scheme 1). Enzyme-mediated deprotonation of the O2 hydroxyl group would permit electron flow toward the N1 atom to create the nucleophile responsible for the attack at the C1 position of the PRPP molecule. An inspection of the structure of our ternary complex shows that the two ordered water molecules that interact with the O2 atom of OA lie within 15° of the ring plane, consistent with hydrogen bonds to the sp^2-hybridized lone pairs present on a keto oxygen (Figure 3B). One of these water molecules is held in position through hydrogen bonds to Lys76 (d_{avg} = 2.7 Å), Lys109 (d_{avg} = 2.9 Å), and the 2′-hydroxyl group of PRPP (d_{avg} = 2.9 Å) and is close to the N1 atom of orotate (d_{avg} = 3.8 Å) and to Asp132 (d_{avg} = 3.3 Å). An identically positioned water molecule is also found in the closed *Salmonella* enzyme ternary complex structure (1LH0).[2] On the basis of the water molecules' proximity to these critical groups, they are likely to mediate the proton transfer necessary for tautomeric conversion at C2 and general base activation. While it is not yet possible to precisely identify the ultimate proton acceptor, it is reasonable to speculate that the immediate acceptor is probably the water molecule in close contact with Lys109, Lys76, or Asp132 or possibly even the departing Mg-diphosphate product, all of which are less likely to perform this role at pH 4.6 (Scheme 1). Mutation of Lys73 in *S. typhimurium* (Lys76 in *S. cerevisiae*) or of Asp132 in *S. cerevisiae* to alanine is associated with a 100-fold decrease in specific activity, with smaller changes in the K_m for

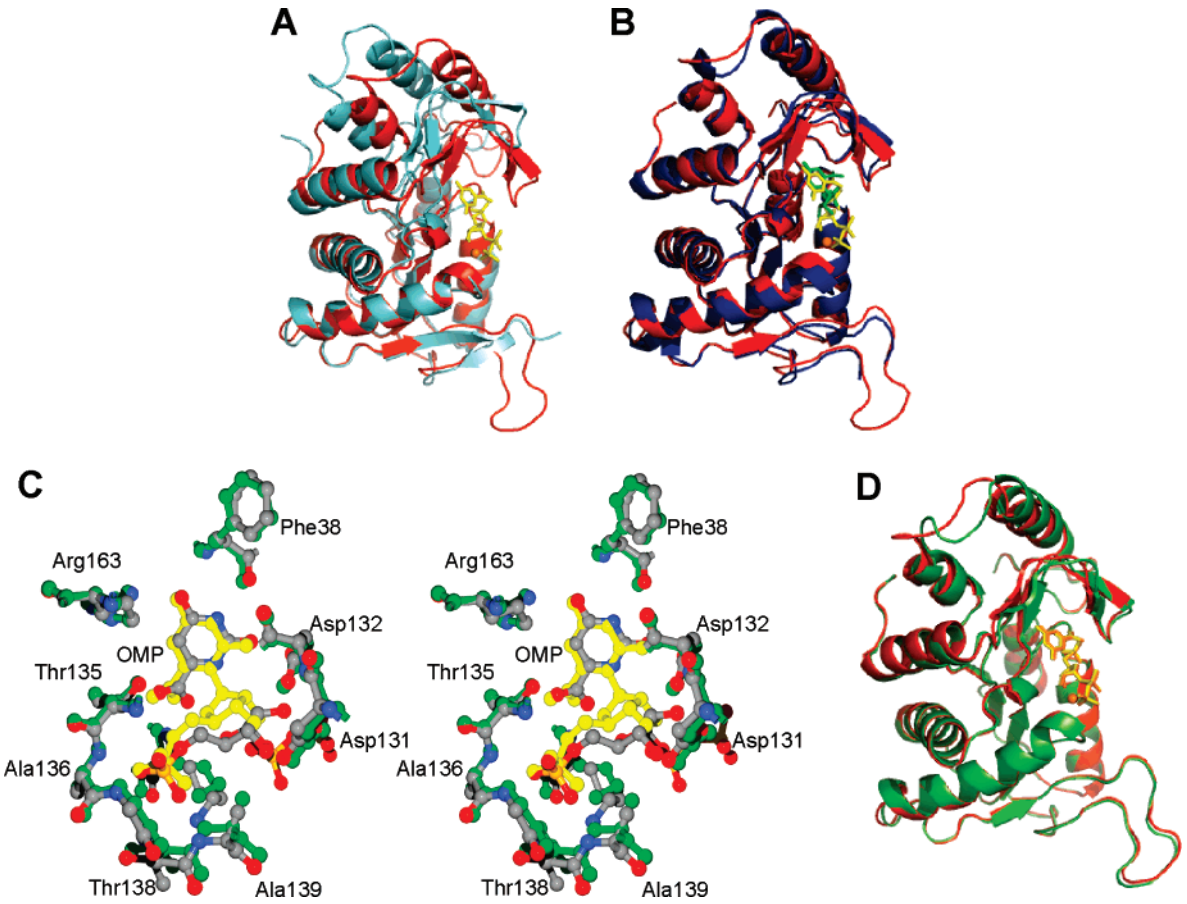

FIGURE 6: Superimposition of *S. cerevisiae* OPRTase structures. (A) Best alignment between the fixed domains of the apo-OPRTase (cyan) and ternary complex (red) structures. (B) Best alignment between the fixed domains of the ternary (red) and binary (blue) complex structures. OMP is colored green; OA and PRPP are colored yellow; magnesium bound in the ternary complex is colored orange and in the binary complex is colored magenta. (C) Superposition of the bound OMP (atom-type coloring) and OA/PRPP (atom-type coloring) molecules based on the best structure alignment of the Cα atoms in each structure (same alignment as in panel B). (D) Superimposition of A (red) and B (green) subunits from the ternary complex structure by use of the positions of their respective fixed domains as the basis for the alignment. OA, PRPP, and magnesium are colored yellow in the A subunit and orange in the B subunit.

substrates, while mutation of Lys103 in the *S. typhimurium* enzyme (Lys109 in *S. cerevisiae*) resulted in a ~1000-fold decrease in k_{cat} (*40*; Table 2). Although neither study can be used to define a specific role for these amino acids, these results are consistent with their greater involvement in the catalytic event than in substrate binding.

In addition to a possible role as a general acid/base catalyst, the positioning of the highly conserved Asp131 and Asp132 residues suggests another role, namely, stabilization of the ribosyl group during catalysis as it changes puckering from 2-endo to 2-exo as a result of inversion at the C1 position. In our ternary complex, Asp131 forms a hydrogen bond with the 3-hydroxyl group and Asp132 forms a hydrogen bond with the 2-hydroxyl group. However, in the OMP complex only Asp132 interacts directly with the ribosyl group, by forming a hydrogen bond with the 3′-hydroxyl. Consequently, it is likely that, in the transition state, these aspartates help to guide the ribosyl group along the reaction trajectory and facilitate the conformational changes within the ring required for the catalytic event. Mutation of either residue to Ala is associated with >100-fold decreases in specific activity, while the double (D → A) mutation results in a 1000-fold reduction in reaction velocity. The fact that neither mutation is associated with more than 3-fold changes in the K_m for PRPP suggests that the interactions contributed by these aspartates are minimal in the ground-state substrate complexes but become more influential during the progression to and from the transition state.

Another likely component to stabilization of the transition state in OPRTase is the Mg^{2+} bound to the PRPP molecule and indirectly to the enzyme through a coordinating water molecule to Asp131. The Mg^{2+} required for catalysis (*34*) likely provides charge stabilization to the departing PP_i, thus increasing the electrophilic nature of the C1 atom through its electron-withdrawing capacity by coordination of the O1 atom of the PP_i group (Figure 5 and Scheme 1). In addition, the coordination of the 2- and 3-hydroxyl groups and the β-phosphate likely provide conformational stability for the relatively flexible PRPP molecule, thereby increasing the likelihood of a productive encounter with the N1 atom of the OA molecule (*36*). Studies have shown that Mg^{2+} typically adopts an octahedral coordination environment in protein structures (*41*), and that is the case in our ternary complex, where four of the six coordinations are provided by PRPP and the remaining two involve ordered water molecules. Many Mg^{2+} binding enzymes possess a sequence motif -Xh-Xh-Xh-Xh-D- associated with binding of the metal, where Xh is any hydrophobic residue and D is a coordinating aspartate residue (*42*). The four residues generally form a β-strand with the key Asp residue lying at the

Scheme 1: Proposed Chemical Mechanism for OPRTase[a]

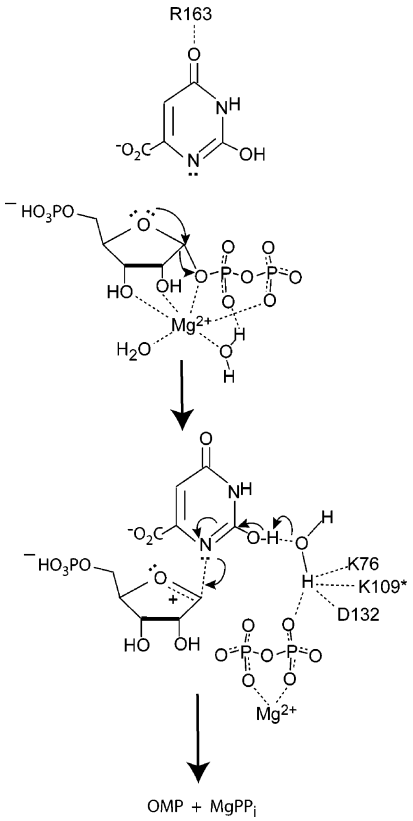

[a] In particular are shown possible involvement of subunit residues (K76 and D132), intersubunit residue (K109*), or diphosphate in activation of water as the general base.

end of the β-strand. Mg^{2+} usually interacts directly with this aspartic acid residue, but it could have indirect interactions with water molecules (*43*). In the case of OPRTase, the Mg^{2+} binding motif is represented by residues 127−131, which comprise the third β-strand of the Rossmann-fold (residues 120−124 in *S. typhimurium*).

In the ternary complex structure the Mg^{2+} ion has six interactions: two involve the ribose hydroxyls, another two involve PP_i oxygens, and the final two coordinations involve water molecules (Figure 5). One of these waters is, in turn, bound to the carboxylate of Asp131, similar to what is observed in the *S. typhimurium* enzyme, where the Mg^{2+} appears to interact indirectly with atoms of the protein via intermediate ordered water (*13*). Interactions identical to those observed in our ternary complex structure were found for Mg^{2+} in human HGPRTase (*35*) and *E. coli* GPATase (PDB code 1ECC) (*16*). In addition, in the *T. cruzi* HPRT structure, one of the metal ions bound to the subunit with a closed conformation has very similar interactions to those observed in our structure of *S. cerevisiae* OPRTase (*37*). Thus, the catalytic magnesium ion interacts with PRPP in a very similar, if not identical, manner in all type 1 PRTases for which structures are available. A second metal ion is found in the HPRT structure, where it appears to perform a role similar to that of Lys109 in the *S. cerevisiae* OPRTase structure and Lys103 in the *S. typhimurium* structure (1LH0).[2]

Prior work showed that the *S. cerevisiae* OPRTase enzyme can bind only one mole of OMP or PRPP in the two apparently identical subunits in a highly cooperative fashion and that the kinetics of the enzyme are inconsistent with the existence of free enzyme once catalytic cycles are initiated (*10*). The structures of OPRTase reported here show that monomers A and B are not identical in the ternary complex due to a difference in the motion of the hood domain between the two subunits (Table 3, Figure 6D). The areas of divergence are in the N-terminal (residues 2−25) and C-terminal (residues 198−223) regions. In addition, a comparison of the four monomers in the OMP complex reveals that A and C as well as B and D are almost identical, with rms differences for Cα atoms of 0.29 and 0.19 Å, respectively. However, if we compare the monomers A to B and C to D, the differences are larger due to a 2° rigid body rotation of their respective hood domains (residues 3−19 and 202−224); rms differences for all Cα-atoms are 0.37 and 0.45 Å, respectively. This structural asymmetry does not appear to be pre-existent in the enzyme. Rather it is associated with ligand binding, since the apoenzyme has exact crystallographic symmetry between the monomers in the functional dimer. While the structural asymmetry present in our ternary and binary complexes is consistent with the available kinetic data that demonstrate nonequivalence of and cooperativity between the subunits for the *S. cerevisiae* OPRTase enzyme, the extent of asymmetry observed in the crystal structures is not as large as the kinetic data suggests. However, striking asymmetry is manifest in the *Salmonella* OPRTase ternary complex structure (1LH0), wherein one active site is nearly catalytically poised, with the loop from the opposing subunit closed over the PRPP and OA; while only OA is bound in the other site with its opposing subunit's loop unstructured.[2] In accord with this crystallographic result, the presence of saturating OA (thus 2 equiv of OA presumably bound) allows for only 1 equiv of PP_i to bind to the dimeric enzyme (*44*) in a dead-end complex. Such a result is indeed consistent with the proposed binding and kinetic scheme for the *Saccharomyces* enzyme, which displays half-of-sites binding of PRPP and OMP (*10*) thus implying half-of-sites reactivity. On the other hand, it is hard to reconcile this asymmetric structure for the *Salmonella* enzyme with the kinetic work, which reported that the *Salmonella* enzyme displays single classes of sites with nearly $n = 2$ binding for both OMP ($n = 1.63$) and PRPP ($n = 1.71$) (*44*).

So why does the ternary complex of the *Saccharomyces* enzyme reported here contain two apparently equivalently bound molecules of PRPP and OA? There are several plausible explanations, but the most compelling is that while the structure observed in the crystal is representative of at least one of the conformational states present in solution, it is not necessarily representative of all or even the major conformational state present in solution. The forces involved in stabilizing lattice formation are sufficient to induce subtle changes in protein structure and shift the equilibrium between conformational states with relatively low energetic barriers (1−3 kcal/mol). For example, when half-the-sites behavior of thymidylate synthase from *Pneumocystis carinii* was correlated to a crystal structure of the dimeric enzyme in which both subunits contained dUMP but only one contained the folate analogue, this paradigmatic demonstration was characterized as "unique" (*45*) in that the enzyme displays half-the-sites reactivity throughout evolution, yet most of the ternary complexes show full site occupancy with some degree of asymmetry (*45*). Indeed several other examples of negative cooperativity were identified where the crystal structures

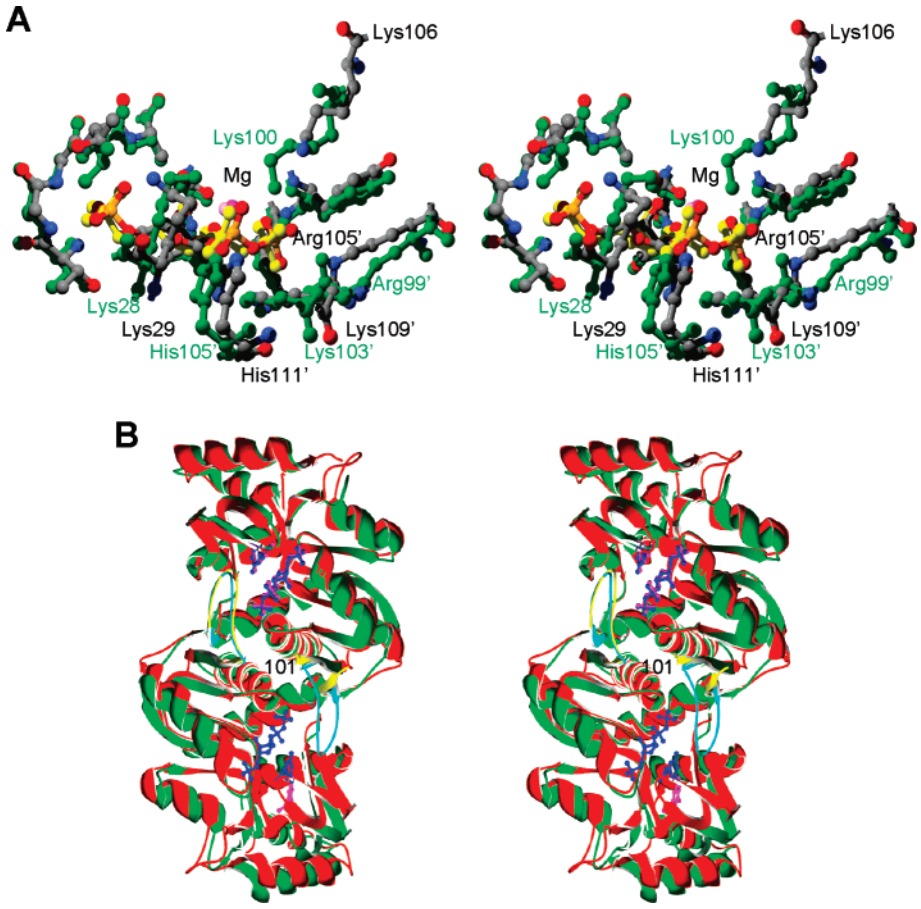

FIGURE 7: Superimposition of *S. cerevisiae* and *S. typhimurium* OPRTase ternary complex structures. (A) OPRTase from *S. typhimurium* (green) showing the interactions surrounding PRPP (yellow) and Mg^{2+} (pink) overlaid onto OPRTase from *S. cerevisiae*, where the amino acids and PRPP are displayed with atom-type coloring and the Mg^{2+} is colored magenta. Labels for the equivalent amino acids in the *S. typhimurium* (green) and *S. cerevisiae* (black) enzymes are provided. (B) Best-fit overlay of the dimeric structures of *S. typhimurium* (green) and *S. cerevisiae* (red): flexible loop structures are colored yellow for the *S. typhimurium* enzyme and cyan for the *S. cerevisiae* enzyme. The position of the last ordered residue in the disordered flexible loop structure of the *S. typhimurium* enzyme is labeled (101).

show monomers in the asymmetric units along with fully liganded proteins (*45*), and this appears to be the rule rather than the exception. For OPRTase the "discrepancy" might easily be attributed to the different crystallization conditions. The *Salmonella* enzyme was derived from a solution of "trisodium citrate"[2] without a defined pH value, though one might infer neutral to alkaline pH, whereas our yeast ternary complex was derived from a solution at pH 4.6. It is thus reasonable to consider that a side chain with a pK_a between the pH of our crystals and that of the kinetic studies (pH 7.5), for example, His 111 (His 105 for *Salmonella*) in the flexible loop, might become fully protonated and stabilize the binding of PRPP in the crystal structure to the point where the participation of Lys106 is unnecessary (see below) and full-site occupancy is induced. Indeed, calculations with the KNF sequential model (*46*) show that a $\Delta\Delta G_{bind}$ of only about 1.5 kcal is required to effect half-of-sites binding in a dimeric enzyme and so any event equal to that in magnitude, such as the changes in protonation state of the pyrophosphate and/or the histidine side chain, could obliterate the effect. What is clear is that the available structures of OPRTase enzymes do not show a strong correlation between ligand stoichiometry observed in the crystalline and solution states but do provide complementary views of substrate binding and the conformational changes that occur during catalysis.

A close inspection of the *Saccharomyces* ternary complex through structural alignment with the cognate *Salmonella* complex (1LH0) reveals that Lys100 in the *Salmonella* enzyme has moved 2.6 Å closer to the diphosphate of PRPP than for the corresponding Lys106 in *Saccharomyces* (Figure 7A). The overall structure of the *Salmonella* enzyme appears more "closed" (24° of closure versus its apoenzyme structure; 1STO), or at least there are more contacts to the diphosphate than observed in our ternary complex (Figure 7B), perhaps depicting a complex much closer to the actual catalytic event. One also notices that, in order to accomplish the movement toward the diphosphate, the main-chain atoms of residues 99−101 have moved ~2.5 Å toward the PRPP in this subunit and away from the opposing subunit (Figure 7). This conformational change would be incompatible with maintaining contacts between amino acids within this loop and a bound PRPP in the opposing subunit since the movement of Lys100 toward PRPP in this subunit would move Arg99, Lys103, and His105 away from the opposing active site. Consequently, this fully engaged structure may reveal an order of events in binding, catalysis, and release of products that is consistent with our kinetic data on the *Saccharomyces* enzyme (*10*), as well as with kinetic data from the *Salmonella* enzyme (*44*). With the asymmetric 1LH0 structure as a starting point, it is tempting to speculate that in order to fully

Scheme 2: Possible Relationship between Conformational States of OPRTase and Kinetic Asymmetry of the Reaction[a]

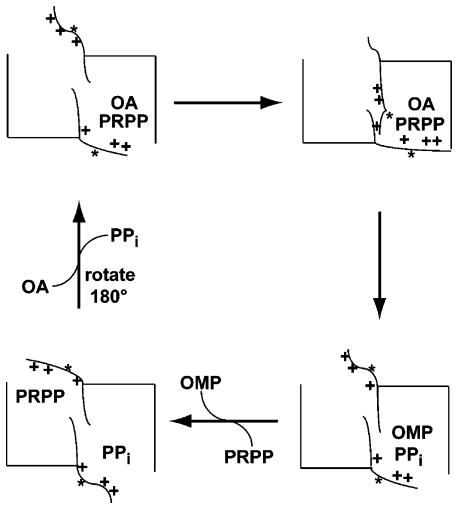

[a] (+) Loop motions depicted with intersubunit contact residues R105, K109, and H111; (*) intrasubunit contact residue K106.

close the active-site loop and engage the side chain of Lys100/106 with the diphosphate in one active site, the loop must be pulled away from the active site of the opposing subunit, thereby promoting the release of its products (at least Mg^{2+}/PP_i), and decreasing the probability of binding PRPP within that active site. Thus, OPRTase would be left with one subunit that can bind at most OMP and another that can bind both reactants: precisely the kinetic scenario we found for the *S. cerevisiae* enzyme. It is intriguing that Arg99/105 and Lys100/106 in each loop contacts the diphosphate of PRPP but in different subunits. Thus, the path for communicating the occupancy of the PRPP site across the subunit interface is effectively reduced to the length of the peptide bond between these residues in each of the two loops. Since the two subunits must communicate with each other through these mobile loops in order to orchestrate the kinetically observed half-the-sites reactivity, we offer Scheme 2 as a kinetic/structural mechanism consistent with all the available kinetic and structural data.

CONCLUSIONS

The active site of the binary and ternary complexes (open and closed structures, respectively) described here provides a clear structural picture of the enzymatic intermediates in the catalytic process in type I PRTases. This work reveals large conformational transitions that occur between the apoenzyme structure and those of the substrate and product complexes. These changes include a rotation of the upper hood domain down onto the bound substrates or products and an ordering of the conserved flexible loop in the substrate ternary complex. The domain rotation and the closed conformation of the flexible loop allow Arg105, Lys109, and His111 to form interactions with the α- and β-phosphate oxygens of PRPP in the companion subunit. These conformational changes are essential to close the active site to bulk solvent molecules, which would lead to unproductive reactions of the oxocarbenium ion transition state. Our structure reveals that OA and Mg^{2+}-PRPP in the ternary complex are oriented for proper attack of the N1 atom on the C1 atom of the ribose ring. The results of the structure determination for the apoenzyme along with the binary and ternary complexes provide new information regarding the active site of the *S. cerevisiae* OPRTase in open and closed conformations that furthers understanding of the OPRTase catalytic mechanism. These structures, combined with a highly asymmetric structure of OPRTase from *S. typhimurium*, provide an explanation for the functional nonequivalence of the active sites, which have been revealed by prior kinetic results (*10*) wherefrom a "double Theorell−Chance" mechanism involving alternating sites catalysis was deduced. In particular, it is possible that complete closure of the active site and engagement of Lys100/106 in the flexible loop with the PRPP in the opposing subunit is a structural sensor that permits alternating cycles of catalysis within the subunits of the dimer.

ACKNOWLEDGMENT

We thank Ms. Kristen Parks, Ms. Amrita Sahota, and Mr. Edward A. Holets for contributions to this project.

REFERENCES

1. Chu, E., and Takimoto, C. H. (1993) in *Cancer: Principles & Practice of Oncology* (De Vita, V. T., Jr., Hellman, S., and Rosenberg, S. A., Eds.) 4th ed., Vol. 1, pp 362−365, Lippincott, Philadelphia, PA.
2. Suttle, J. P., Becroft, D. M. O., and Webster, D. R. (1989) in *The Metabolic Basis of Inherited Disease* (Scriver, C. R., Beaudet, A. L., Sly, W. S., and Valle, D., Eds.) 6th ed., pp 1095−1126, McGraw-Hill, New York.
3. Simmonds, H. A., Sahota, A. S., and Van Acker, K. J. (1989) in *The Metabolic Basis of Inherited Disease* (Scriver, C. R., Beaudet, A. L., Sly, W. S., and Valle, D., Eds.) 6th ed., pp 1029−1044, McGraw-Hill, New York.
4. Stout, J. T., and Caskey, C. T. (1989) in *The Metabolic Basis of Inherited Disease* (Scriver, C. R., Beaudet, A. L., Sly, W. S., and Valle, D., Eds.) 6th ed., pp 1007−1028, McGraw-Hill, New York.
5. Ullman, B., and Cater, D. (1995) Hypoxanthine-guanine phosphoribosyltransferase as a therapeutic target in protozoal infections, *Infect. Agents Dis. 4*, 29−40.
6. Kanaani, J., Maltby, D., Somoza, J. R., and Wang, C. C. (1997) Inactivation of *Tritrichomonas foetus* and *Schistosoma mansoni* purine phosphoribosyltransferases by arginine-specific reagents, *Eur. J. Biochem. 244*, 810−817.
7. Goitein, R. K., Chelsky, D., and Parsons, S. (1978) Primary ^{14}C and alpha secondary ^{3}H substrate kinetic isotope effects for some phosphoribosyltransferases, *J. Biol. Chem. 253*, 2963−2971.
8. Victor, J., Greenberg, L. B., and Sloan, D. L. (1979) Studies of the kinetic mechanism of orotate phosphoribosyltransferase from yeast, *J. Biol. Chem. 254*, 2647−2655.
9. Witte, J. F., Tsou, R., and McClard, R. W. (1999) Cloning, overproduction, and purification of native and mutant recombinant yeast orotate phosphoribosyltransferase and the demonstration from magnetization inversion transfer that a proposed oxocarbocation does not have a kinetic lifetime, *Arch. Biochem. Biophys. 361*, 106−112.
10. McClard, R. W., Holets, E. A., MacKinnon, A. L., and Witte, J. (2006) Half-of-sites binding of orotidine 5′-phosphate and α-D-5-phosphorylribose 1-diphosphate to orotate phosphoribosyltransferase from *Saccharomyces cerevisiae* supports a novel variant of the Theorell-Chance mechanism with alternating site catalysis, *Biochemistry 45*, 5330−5342.
11. Bhatia, M. B., Vinitsky, A., and Grubmeyer, C. (1990) Kinetic mechanism of orotate phosphoribosyltransferase from *Salmonella typhimurium*, *Biochemistry 29*, 10480−10487.
12. Scapin, G., Grubmeyer, C., and Sacchettini, J. C. (1994) Crystal structure of orotate phosphoribosyltransferase, *Biochemistry 33*, 1287−1294.
13. Scapin, G., Ozturk, D. H., Grubmeyer, C., and Sacchettini, J. C. (1995) The crystal structure of the orotate phosphoribosyltransferase complexed with orotate and α-D-5-phosphoribosyl-1-pyrophosphate, *Biochemistry 34*, 10744−10754.

14. Wang, G. P., Cahill, S. M., Liu, X., Girvin, M. E., and Grubmeyer, C. (1999) Motional dynamics of the catalytic loop in OMP synthase, *Biochemistry 38*, 284−295.
15. Smith, J. L. (1999) Forming and inhibiting PRT active sites, *Nat. Struct. Biol. 6*, 502−504.
16. Krahn, J. M., Kim, J. H., Burns, M. R., Parry, R. J., Zalkin, H., and Smith, J. L. (1997) Coupled formation of an amidotransferase interdomain ammonia channel and a phosphoribosyltransferase active site, *Biochemistry 36*, 11061−11068.
17. Bradford, M. M. (1976) A rapid and sensitive method for the quantitation of microgram quantities of protein utilizing the principle of protein-dye binding, *Anal. Biochem. 72*, 248−256.
18. Pflugrath, J. W. (1999) The finer things in X-ray diffraction data collection, *Acta Crystallogr. D55*, 1718−1725.
19. Otwinowski, Z., and Minor, W. (1997) Processing of X-ray diffraction data collected in oscillation mode, *Methods Enzymol. 276*, 307−326.
20. Navaza, J. (1994) *AMoRe*: an automated package for molecular replacement, *Acta Crystallogr. A50*, 157−163.
21. Vagin, A., and Teplyakov, A. (1997) MOLREP: an automated program for molecular replacement, *J. Appl. Crystallogr. 30*, 1022−1025.
22. Collaborative computational project, Number 4 (1994) The CCP4 suite: Programs for protein crystallography, *Acta Crystallogr. D50*, 760−763.
23. Brünger, A. T., Adams, P. D., Clore, G. M., DeLano, W. L., Gros, P., Grosse-Kunstleve, R. W., Jiang, J.-S., Kuszewski, J., Nilges, N., Pannu, N. S., Read, R. J., Rice, L. M., Simonson, T., and Warren, G. L. (1998) *Crystallography and NMR System*: A new software system for macromolecular structure determination, *Acta Crystallogr. D54*, 905−921.
24. Jones, T. A., Zhou, J. Y., Cowan, S. W., and Kjeldgaard, M. (1998) Improved methods for building protein models in electron density maps and the location of errors in these models, *Acta Crystallogr. A47*, 110−119.
25. Emsley, P., and Cowtan, K. (2004) Coot: model-building tools for molecular graphics, *Acta Crystallogr. D60*, 2126−2132.
26. Kleywegt, G. J., and Jones, T. A. (1998) Databases in protein crystallography, *Acta Crystallogr. D54*, 1119−1131.
27. Hayward, S., and Berendsen, H. J. C. (1998) Systematic analysis of domain motions in proteins from conformational change: New results on citrate synthase and T4 lysozyme, *Proteins: Struct., Funct., Genet. 30*, 144−154.
28. Kabsch, W. (1976) A solution for the best rotation to relate two sets of vectors, *Acta Crystallogr. A32*, 922−923.
29. DeLano, W. L. (2002) The PyMOL Molecular Graphics System on World Wide Web, http://www.pymol.org.
30. Guex, N., and Peitsch, M. C. (1997) SWISS-MODEL and the Swiss-PdbViewer: An environment for comparative protein modeling, *Electrophoresis 18*, 2714−2733.
31. Cason, C. J. (1999) *POV-Ray for Windows*, version 3.1, http://www.povray.org/.
32. De Montigny, J., Belarbi, A., Hubert, J. C., and LaCroute, F. (1989) Structure and expression of the URA5 gene of *Saccharomyces cerevisiae*, *Mol. Gen. Genet. 215*, 455−462.
33. Branden, C., and Tooze, J. (1991) *Introduction to protein structure*, Garland Publishing, Inc., New York.
34. Bhatia, M. B., and Grubmeyer, C. (1993) The Role of Divalent Magnesium in Activating the Reaction Catalyzed by Orotate Phosphoribosyltransferase, *Arch. Biochem. Biophys. 303*, 321−325.
35. Balendiran, G. K., Molina, J. A., Xu, Y., Torres-Martínez, J., Stevens, R., Focia, P. J., Eakin, A. E., Sacchettini, J. C., and Craig, S. P., III (1999) Ternary complex structure of human HGPRTase, PRPP, Mg^{2+}, and the inhibitor HPP reveals the involvement of the flexible loop in substrate binding, *Protein Sci. 8*, 1023−1031.
36. Henriksen, A., Aghajari, N., Jensen, K. F., and Gajhede, M. (1996) A flexible loop at the dimer interface is a part of the active site of the adjacent monomer of *Escherichia coli* orotate phosphoribosyltransferase, *Biochemistry 35*, 3803−3809.
37. Focia, P. J., Craig, S. P., III, and Eakin, A. E. (1998) Approaching the transition state in the crystal structure of a phosphoribosyltransferase, *Biochemistry 37*, 17120−17127.
38. Chelsky, D., and Parsons, S. (1975) Stereochemical course of the adenosine triphosphate phosphoribosyltransferase reaction in histidine biosynthesis, *J. Biol. Chem. 250*, 5669−5673.
39. Tao, W., Grubmeyer, C., and Blanchard, J. S. (1996) Transition state structure of *Salmonella typhimurium* orotate phosphoribosyltransferase, *Biochemistry, 35*, 14−21.
40. Ozturk, D. H., Dorfman, R. H., Scapin, G., Sacchettini, J. C., and Grubmeyer, C. (1995) Locations and functional roles of conserved lysine residues in *Salmonella typhimurium* orotate phosphoribosyltransferase, *Biochemistry 34*, 10755−10763.
41. Castagnetto, J. M., Hennessy, S. W., Roberts, V. A., Getzoff, E. D., Tainer, J. A., and Pique, M. E. (2002) MDB: the Metalloprotein Database and Browser at The Scripps Research Institute, *Nucleic Acids Res. 30*, 379−382.
42. Black, M. E., and Hruby, D. E. (1992) Site-directed mutagenesis of a conserved domain in vaccinia virus thymidine kinase. Evidence for a potential role in magnesium binding, *J. Biol. Chem. 267*, 6801−6806.
43. Harmark, K. M., Anborgh, P. H., Merola, M., Clark, B. F. C., and Parmeggiani, A. (1992) Substitution of aspartic acid-80, a residue involved in coordination of magnesium, weakens the GTP binding and strongly enhances the GTPase of the G domain of elongation factor Tu, *Biochemistry 31*, 7367−7372.
44. Wang, G. P., Lundegaard, C., Jensen, K. F., and Grubmeyer, C. (1999) Kinetic mechanism of OMP synthase: a slow physical step following group transfer limits catalytic rate, *Biochemistry 38*, 275−283.
45. Anderson, A. C., O'Neil, R. H., DeLano, W. L., and Stroud, R. M. (1999) The Structural Mechanism for Half-the-Sites Reactivity in an Enzyme, Thymidylate Synthase, involves a Relay of Changes between Subunits, *Biochemistry 38*, 13829−13836.
46. Koshland, D. E., Jr., Nemethy, G., and Filmer, D. (1966) Comparison of Experimental Binding Data and Theoretical Models in Proteins Containing Subunits, *Biochemistry 5*, 365−385.

BI701023Z